Preprint (full version: SPIE Proceedings 2012)

Numerical Modelling and *In Vivo* Analysis of Fluorescent and Laser Light Backscattered from Glial Brain Tumors

Tatiana A. Savelieva[a], Nina A. Kalyagina[*a], Maria N. Kholodtsova[a], Victor B. Loschenov[a], Sergey A. Goryainov[b], and Alexander A. Potapov[b]
[a]Prokhorov General Physics Institute, Russian Academy of Sciences, 119991,Russia, Moscow, Vavilov Str.;
[b]Burdenko Neurosurgery Institute, 125047, Russia, Moscow, 4th Tverskaya-Yamskaya Str., 16

ABSTRACT

Brain glial tumors have peculiar features of the perifocal region extension, characterized by its indistinct area, which complicates determination of the borders for tissue resection. In the present study filter-reduced back-scattered laser light signals, compared to the data from mathematical modeling, were used for description of the brain white matter. The simulations of the scattered light distributions were performed in a Monte Carlo program using scattering and absorption parameters of the different grades of the brain glial tumors. The parameters were obtained by the Mie calculations for three main types of scatterers: myelinated axon fibers, cell nuclei and mitochondria. It was revealed that diffuse-reflected light, measured at the perifocal areas of the glial brain tumors, shows a significant difference relative to the signal, measured at the normal tissue, which signifies the possibility to provide diagnostically useful information on the tissue state, and to determine the borders of the tumor, thus to reduce the recurrence appearance. Differences in the values of ratios of diffuse reflectance from active growth parts of tumors and normal white matter can be useful for determination of the degree of tumor progress during the spectroscopic analysis.

Keywords: tissue light scattering, brain glial tumor, Monte Carlo simulation, Mie scattering, fluorescence spectra, optical properties, biological scatterers.

1. INTRODUCTION

The main cause of recurrence of glial brain tumors after neurosurgical removal is an extensive infiltration of tumor cells to the normal white matter. Fast spectroscopic detection of structural and biochemical abnormalities of tumoral and adjacent glial tissues during the neurosurgical procedure is a way to attain eradication of tumor with the most possible preservation of normal white matter.

Glial tumors are characterized by complex alterations, both in metabolic state of the tissue and structural changes at different levels of tissular and cellular organization. To quantify accurately such changes one has to elucidate the state of normal subcortical white matter and glial tumors of different grades. Glial brain tumors grow along the myelinated fiber tracts throughout the normal white matter without establishing any capsule[1]. They consist of a core mass and a perifocal area[2, 3], with progression of displacement, deviation, and destruction of the myelinated fiber tracts[4] with tumor extension. The core of glioblastoma multiforme, the most malignant glial tumor, is characterized by the central necrosis and thus destructive changes in the myelinated axon fibers[5, 6]. Tumors without central necrosis and edema in the perifocal areas, such as low-grade gliomas (grade II by World Health Organization (WHO)) or high-grade anaplastic gliomas (WHO grade III), often appear to have relatively constant within the tumor center or tumor border[4]. Increase in the blood content in the tumoral tissues is a typical feature for gliomas[7]. The cellular composition of glioblastoma multiforme (WHO Grade IV) appears hypercellular, with nuclear atypia and size growth, and pleomorphism[8]. Anaplastic astrocytoma, placed in the grading systems closer to malignant end, characterized by cellular tightness, anaplasia, and mitoses with a less pronounced extent than at glioblastoma. Low-grade astrocytoma exhibits moderate hypercellularity and nuclear size enlargement without cellular atypia and mitotic activity Pilocytic astrocytoma is a sparsely hypercellular tumor without anaplasia or mitoses, consisting of cellular and fibrillary perivascular areas [9, 10].

At the subcellular level the most dramatic changes were observed on the structure and content of mitochondria in the glial tumors. Mitochondria provide most of the energy for brain cells by the oxidative phosphorylation. In normal brain tissues mitochondria occupy about 7-8% of the cell volume[11, 12]. The Warburg effect (revealed in cancer cells predominantly producing energy by a high rate of glycolysis followed by lactic acid fermentation in the cytosol, rather than by a relatively low rate of glycolysis followed by the oxidation of pyruvate in mitochondria) demonstrates the transition of the energetic supply from mitochondria to non-oxidizing decomposition of glucose, which, together with cell progressive destruction, leads to diminution at the sizes and quantity of mitochondria, as well as their restructure in tumor cells. Several works devoted to the structural analysis of mitochondria in the cells of astrocytic tumors by the electron microscopy[13, 14], has shown a high heterogeneity of mitochondrial disposition, partial or total cristolysis, and reduction of number of mitochondria in the tumor cells. The analysis of activities of two unrelated mitochondrial enzymes, cytochrome c oxidase (COX IV) and citrate synthase in glioma homogenates, carried out by Outard *et al.*[14], also has demonstrated the decrease in mitochondrial content of glioma in comparison with the normal rat brain tissue. The investigation of mitochondrial content in 26 samples of glioma and 9 samples of normal white matter by the confocal microscopy[15] has observed the significant reduction of the COX IV of about 15.3 times ($P < 0.01$) in the tumor tissues comparably with normal white matter.

One of the most interesting from the diagnostic point of view alterations at the tumor metabolism, is the decrease of ferrochelatase level that results the accumulation of the protoporphyrin IX in the rapidly proliferating tumor cells after the 5-aminolevulinic acid administration. The ability of the protoporphyrin IX to fluoresce explains its active use as the natural metabolite, induced by the 5-aminolevulinic acid (5-ALA), for fluorescent marking of tumor tissue during the neurosurgical diagnostic and navigative procedures. The studies on correlation between the level of accumulation of the protoporphyrin IX and the tumor grade allowed to reveal that low-grade gliomas accumulate the protoporphyrin-IX in a concentration of about 0.0034 μg/ml[16] which is much smaller than the sensitivity limit of conventional fluorescence video devices, thus require additional diagnostic analysis. The present study presents a method of differentiation of low- and high-grade gliomas from normal tissue by means of a complementary analysis of diffusely reflected laser light from the tissue.

The nature of the main scatterers of biological tissue is a complex phenomenon. The analysis of liver slices by the phase-contrast microscopy[17] has shown that the spectrum of the spatial frequencies of fluctuations of refractive index shows a power-law behavior spanning at least a decade (0.5-5 μm^{-1}). This range of the spatial frequencies corresponds to the range of the scatterer‘s sizes from 0.2 to 2 μm. A discrete particle model, introduced by Schmitt *et al.*[18], assumed that the variations in the refractive-indices, caused by microscopic tissue elements, can be treated as the variations in the sizes of the particles distributed according to the skewed log-normal function. The analysis of scatterer’s size distribution based on the Mie theory was also performed resulting on the measurements of angular dependence of light scattering by biological cells[19]. Basing on the sizes of scatterers and scattering cross sections, it was shown that the best compliance with the experiment for the log-normal distribution is at the maximum near 2 μm. However, the morphological correlates of the scattering by biological tissues are still under investigation.

The studies of Beauvoit *et al*. have shown that in the liver tissues mitochondria have a significant effect on the light scattering[20, 21]. In the experiments with rodent tumors[12] the same authors have demonstrated the strong dependence between light scattering and two markers of mitochondrion content: succinate dehydrogenase activity and mitochondrial protein content. The content of proteins and lipids (main components of the mitochondrial membranes and matrix at a dry form) also defines the refractive indices of the biological medium and hereupon its ability to scatter light[22]. Thus, in accordance with these two observations we can make an assumption about decrease in the scattering intensity as a result of reduction of the mitochondrial content.

Mathematical modeling of light scattering from living cells by the finite-difference time-domain method[23] has demonstrated a large effect of small organelles on the scattering of the pattern. The total amount of the scattered light for a cell with small organelles was 1.7 times greater than for the same cell without them. Another hypothesis asserting that the main contribution to the light scattering from cells is caused by the nucleus and cell membranes was presented by Backman *et al.* [24] and Beuthan *et al.*[25]. In the first work, the conclusion is based on the result of the light scattering spectroscopy of polarized light and analysis of the spectrum of a single backscattering component of the light scattered from cells. In the second work, based on the results of phase-contrast spectroscopy, the obtained data has shown that the single phase shift of the mitochondria was small in comparison with the total phase shift. Thus the nucleus and the membranous structures of the tissue gave the most considerable phase shift of the cell. However, nuclei size of the glial tissue is smaller than of an epithelial one (a usual object of the majority of studies[26]), which reduces their impact to the

scattering. Also, the impact of the myelin, a membranous, lipid, and protein-rich structure[27], has to be taken into account for the analysis of light scattering from glial brain tissue. The dry mass of myelin is characterized by a high proportion of lipid (70-85%) and, consequently, a low proportion of protein (15-30%)[28], which gives such a tissue component a high refractive index. Thus, the main scatterers taken into account in this study are myelinated axon fibers, cell nuclei and mitochondria.

The geometry of measurements, i.e. the distance between the light source and detector, their numerical apertures and distance to the object, also plays an important role at the contribution of different-sized structures to the registered backscattered light. A fiber-optic probe with a distance between the source and detector fibers equal to 250 μm and numerical aperture of 0.37 was used in our clinical studies. In the study of Mourant *et al.* [29] the contribution of different scatterers to the backscattering by Monte-Carlo simulation of light propagation, performed with different forms of the scattering phase function and small numerical aperture of delivering and collecting fibers, was analyzed. Another work[30], carried out on the tissue phantom with different scatterer's sizes, and source-detector separations, has demonstrated the high-angle scattering enhancement at the case of light collection near the delivery fiber. Such specific features of measurements of the back-scattered laser light, as well as the peculiarities of the brain white matter structure at normal and tumorous states will be taken into account in our study.

2. MATERIALS AND METHODS

Necessary for the present study optical characteristics of the main scatterers are: sizes, refractive indices and density. From the histological studies, mean sizes and density of the nuclei (refractive index n = 1.39[35]) for the normal, astrocytomal and glioblastomal tissues were determined. Mitochondria in glial cells appear mostly small[27], with possible size variations from 0.2 to 1.5 μm[36]. Average diameters and density of the myelinated axons of normal white matter were taken from the studies of von Keyserlingk *et al.*[37], and Evangelou *et al.*[38] and Biedenbach *et al.*[39], respectively. Stepwise growth of the number of demyelinated axons, leads to the diminution of mean diameter of the fibers up to axonal diameter, related to the thickness of the myelin sheath by the *g-ratio* which is usually about 0.6[40]. The value of the refractive index also reduces due to the non-myelin axonal consistence, similar to the neuron body, and is about 1.375[41] in a contrast to the refractive index of the myelin sheath (n = 1.455[34]). Besides, most of the studies revealed an increase in the average cosine (g) of scattering from normal tissues to tumorous, and raised absorption coefficient at 530-700 nm in the glial tumors due to the higher blood content[42]. The average values of the absorption coefficients and g were taken according to the data presented in Ref. 42, and their growth was performed at a gradual form from normal tissues to tumorous. The surrounding media for the main scatterers is microglia, extracellular matrix and cellular cytoplasm with relatively low refractive indices due to their consistence. The results of literature analysis and histological studies, described above, are shown in Table 1. In Table 2 the results of the analytical modeling of the optical properties of white matter and brain tumors of different grades are presented.

Table 1. Parameters for Mie calculations. * *indicates the change of the refractive index from the one of the myelin sheath to the axonal one.*

	Center			Perifocal Zone (Border)		
Parameter	**a**, diameter of a scattrer (μm) **nuclei / mitochondria / myelin fibers**	**ρ**, density **nuclei** (per μm^3) / **mitochondria** (per cell) / **myelin fibers** (per μm^3)	**n**, refractive index **nuclei / mitochondria / myelin fibers**	**a**, diameter of a scattrer (μm) **nuclei / mitochondria / myelin fibers**	**ρ**, density **nuclei** (per μm^3) / **mitochondria** (per cell) / **myelin fibers** (per μm^3)	**n**, refractive index **nuclei / mitochondria / myelin fibers**
Normal-Appearing White Matter	2 / 0.5 / 0.8 (100%)	0.0004 / 200 / 0.07	1.39 / 1.42 / 1.455	-		
WHO Grade II-III	3 / 0.3 / 0.8 (40%); 0.48 (60%*)	0.0007 / 70 / 0.07	1.39 / 1.42 / 1.455	2.5 / 0.3 / 0.8 (50%); 0.48 (50%*)	0.0005 / 70 / 0.07	1.39 / 1.42 / 1.455
WHO Grade IV	4.5 / 0.25 / 0.8 (20%); 0.48 (80%*)	0.0015 / 0-30 / 0.07	1.39 / 1.42 / 1.455	3 / 0.25 / 0.8 (40%); 0.48 (60%*)	0.0007 / 30 / 0.07	1.39 / 1.42 / 1.455

Table 2. Parameters for Monte Carlo simulation.

Parameter/ wavelength		**Normal tissue**	**WHO Grade II-III**		**WHO Grade IV**	
			Tumor in active growth area	**Perifocal zone (border)**	**Tumor in active growth area**	**Perifocal zone (border)**
μ_s, cm-1	**632.8 nm**	113.7	49.7	54.2	112.6	50.9
	710 nm	88.4	39.3	42.9	90	40.3
μ_a, cm-1	**632.8 nm**	1.7	3	2.2	7.1	3.5
	710 nm	0.76	2	1.5	2.5	1.2
g	**632.8 nm**	0.85	0.89	0.86	0.9	0.89
	710 nm	0.84	0.88	0.85	0.89	0.88

Monte Carlo modeling of light transport in the brain white matter tissue was used in the present study in order to trace the reflections of the tissue changes in the back-scattering from semi-infinite media, containing scatterers, absorbers and fluorophores.

3. RESULTS AND DISCUSSION

Figure 1 presents an example of the light spectra measured from the perifocal areas and areas of active growth of glioblastoma multiforme. The peak at 632.8 nm was formed by the backscattering of the laser light, while the broad peak with the maximum at 705 nm was formed by the ALA-induced protoporphyrin IX fluorescence. Comparison of the intensities of the backscattered laser and fluorescent light allowed us to perform the simultaneous analysis of the structural and biochemical changes at the same tissue regions. The spectra demonstrate smooth changes of the laser light scattering and fluorescence intensities, changing in opposite directions, for the perifocal and central zones of the tumor. The statistical diagram of the spectroscopic data, in coordinate axes of the laser light scattering and fluorescence intensity, is presented in Figure 2.

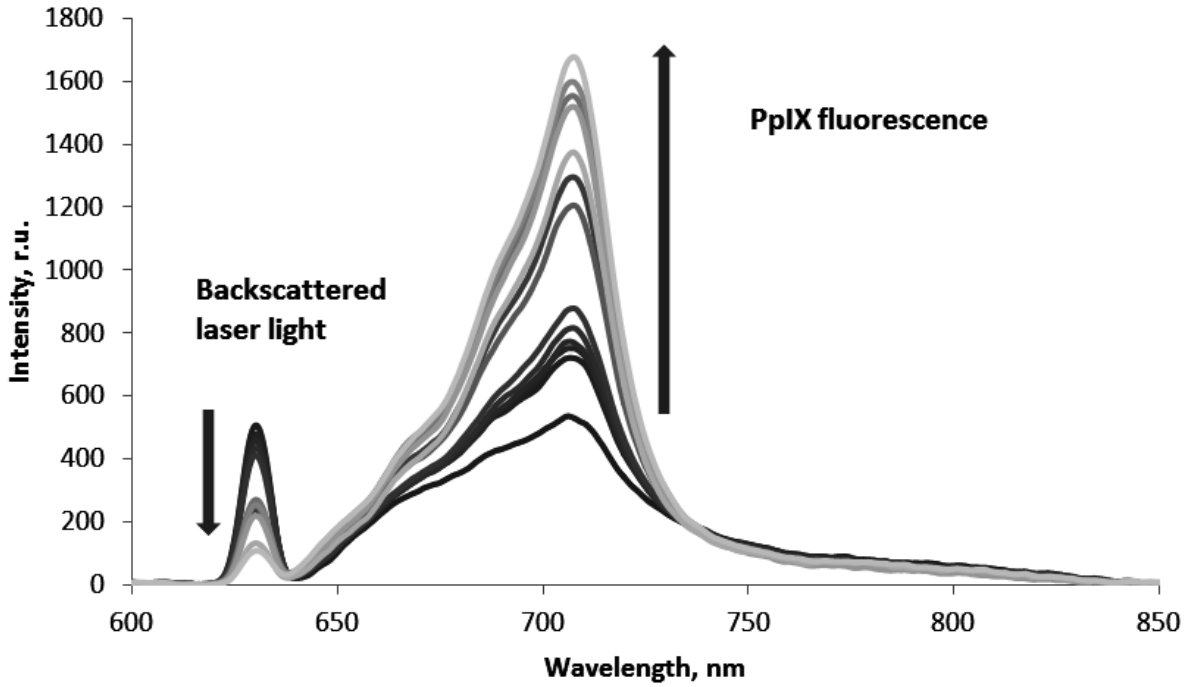

Figure 1. Spectral dependence of attenuated backscattered laser light and fluorescence; the left arrow shows decrease of scattering intensity and the right arrow shows the simultaneous increase of fluorescence signal during sequential spectroscopic in vivo measurements of brain tissue from periphery towards the center of tumor.

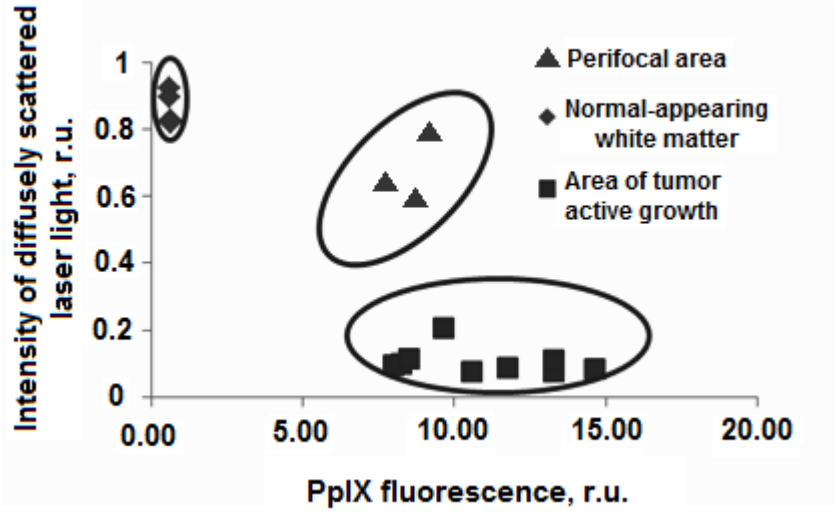

Figure 2. Mapping of the morphological status of tissue in the point of spectroscopic measurement in the coordinate system of backscattered laser light - fluorescence intensity normalized to the respective values of normal-appearing white matter. In the top left corner of the diagram is a cluster of normal-appearing white matter with low dispersion in the scattering properties and almost without dispersion in fluorescence intensity. Along the abscissa - a cluster of tumor tissue formed by high dispersion in fluorescence intensity and lower dispersion in scattering properties. At the main diagonal of the map a cluster of perifocal area usually formatted, which characterized a wide range of scattering and fluorescence changes.

Basing on the histological studies of the tissue zones, at which the diffuse-reflectance (λ = 632.8 nm) was acquired by the optical probe, the obtained signals were classified into three groups for each patient: normal tissues, areas of the tumor active growth and borders, i.e. areas of infiltrative growth of tumor adjoining the healthy white matter. All the obtained signals were normalized by the value for the normal-appearing white matter. The analysis of the intensities of diffuse-reflected laser light revealed statistically non-sufficient differences in the back-scattered laser intensities for the tumors of the WHO Grade II and Grade III. Thus, at the present study the results of simulations and clinical analysis were divided into two categories of the tumor type: astrocytomal (for the low-grade pilocytic astrocytomas and anaplastic astrocytomas) and glioblastomal (high-grade glioblastomas multiforme). Table 3 presents the data obtained from mathematical modeling and clinical trials.

Table 3. Diffuse reflectance signal modelled with Monte Carlo simulations and registered *in vivo* at the laser light wavelength.

Diffuse reflectance normalized to value obtained from normal white matter		**Normal-appearing tissue**	**WHO Grade II-III**		**WHO Grade IV**	
			Tumor in active growth area	**Perifocal zone (border)**	**Tumor in active growth area**	**Perifocal zone (border)**
Rd(MC)	**632.8 nm**	1	0.22±0.00001	0.41±0.00002	0.56±0.00001	0.28±0.00001
Rd(*in vivo*)		1	0.21±0.02	0.37±0.02	0.53±0.02	0.26±0.02

Different responses on the scattering alterations from the central part to the border of tumor for low-grade and malignant gliomas were observed. As it was previously stated, the fraction of well-structured myelinated fibers in tissue decreases with increase of the tumor grade, as well as from the border to the center of tumor. This leads to attenuation of the scattering intensity, affecting the diffuse reflectance signal, which, in a couple with the absorption changes, makes it higher at the perifocal area than at the area of the tumor active growth at the tumors belonged to the first category (lower grade gliomas). Glioblastoma multiforme has appeared characterizing by the reduced level of diffuse reflectance signal

for the center and the border of tumor. However, the prevalence at cellularity at high-grade tumors in comparison with lower-grade gliomas gave an impact on the scattering properties of the tissue, despite the higher absorption. This explains the growth of the diffuse reflectance signal at the area of active tumor growth for glioblastoma multiforme. Such assessment criterion of high-scale scatterers content in the tissue as fractional anisotropy factor allows to evaluate the integrity of the myelinated fibers in tissue, unlike the cellularity growth that is usually less considered at the diffuse tensor imaging studies, and can be revealed with histological study.

The features of the measurement geometry used in our study explain the necessity of taking into consideration the changes in the mitochondrial content. Owing to the small distance between the source and detecting fibers the impact of small-sized organelles with a more wide-angle scattering phase function to the measured signals was significant. In the study of Beauvoit *et al*.[12] it was shown that scattering coefficient positively correlates with mitochondrial protein content of normal tissues and tumors. Thus the growth of cellularity and the decrease of mitochondrial and myelinated axonal content are competitive processes taking place during the tumor progression. In the present study it was revealed that the mitochondrial impact to the back-scattering of the laser light is significant only at the normal tissues. While the impacts of the myelinated fibers and nuclei cross-intercepts the advantage at the scattering intensity. However, the myelinated fibers show the most stable prevalence at the scattering component for the whole first category of the astrocytomal tumors as well as at the normal tissues. The scattering by the cell nuclei dominates only at the areas of active growth of the glioblastoma multiform, where the nuclear sizes and concentrations are about 2.5 times higher than at the normal white matter.

According to the in vivo measurements on 10 patients (74 tissue samples) and mathematical simulations, statistically significant differences in the normal brain white matter, perifocal zone, and zone of the active tumor growth were found at the level of the back-scattered laser signal. This signifies diagnostically useful information on the tissue state for more accurate determination of the tumor borders during the simultaneously with fluorescence navigation, thus to reduce the recurrence appearance. Such information is the most valuable in the case of the low-grade gliomas, as 2 from 3 fluorescence measurements have not shown the accumulation of the tumor marker. In such cases, the lack in sensitivity of the spectroscopic fluorescence technique leads to non-highly accurate navigation during the neurosurgery procedures. The numerical modeling, describing a character of the cellular and subcellular changes of the brain white matter tissue during the tumor formation, has shown a good agreement with the clinical data.

REFERENCES

[1] Brat D. J., “Mechanisms of tumor progression: angiogenesis, hypoxia, and invasion,” Conf. proceedings of the American Society of Neuroradiology: integration of imaging strategies in neuroradiology, 1-8 (2004).

[2] Giese A., Bjerkvig R., Berens M. E., Westphal M., “Cost of migration: invasion of malignant gliomas and implications for treatment, “ J Clin Oncol 21(8), 1624-1636 (2003).

[3] Tonn J.C, Goldbrunner R. “Mechanisms of glioma cell invasion,” Acta Neurochir Suppl 88,163-167 (2003).

[4] Goebell E., Paustenbach S., Vaeterlein O., Ding X.-Q., Heese O., Fiehler J., Kucinski T., Hagel C., Westphal M., Zeumer H., “Low-Grade and Anaplastic Gliomas: Differences in Architecture Evaluated with Diffusion-Tensor MR,” Imaging, Radiology 239(1), 217-222 (2006).

[5] Brunberg J. A., Chenevert T. L., McKeever P. E., Ross D. A., Junck L. R., Muraszko K. M., Dauser R., Pipe J. G. and Betley A. T., “In vivo MR determination of water diffusion coefficients and diffusion anisotropy: correlation with structural alteration in gliomas of the cerebral hemispheres,” AJNR Am J Neuroradiol 16, 361-371 (1995).

[6] Sinha S, Bastin ME, Whittle IR, Wardlaw JM. “Diffusion tensor MR imaging of highgrade cerebral gliomas”. AJNR Am J Neuroradiol 23, 520-527 (2002).

[7] Aronen H. J., Gazit I. E., Louis D. N., Buchbinder B. R., Pardo F. S., Weisskoff R. M., Harsh G. R., Cosgrove G. R., Halpern E. F. and Hochberg F. H., “Cerebral blood volume maps of gliomas: comparison with tumor grade and histologic findings,” Radiology 191(1), 41-51 (1994).

[8] Candolfi M., Curtin J. F., Nichols W.S., Muhammad A. G., King G. D , Pluhar G. E., McNiel E. A., Ohlfest J. R., Freese A. B., Moore P. F., Lerner J., Lowenstein P. R., Castro M. G., “Intracranial glioblastoma models in preclinical neuro-oncology: neuropathological characterization and tumor progression,” J Neurooncol. 85(2), 133-148 (2007).

[9] Schiffer D., [Brain Tumor Pathology: Current Diagnostic Hotspots and Pitfalls], Springer, The Netherlands, (2006).

[10] Sarkar C, Jain A, Suri V., "Current concepts in the pathology and genetics of gliomas," Indian J Cancer 46(2), 108-119 (2009).
[11] Pysh J. J. and Khan T., "Variations in mitochondrial structure and content of neurons and neuroglia in rat brain: An electron microscopic study", Brain Research 36(1), 1-18 (1972).
[12] Beauvoit B., Evans S. M., Jenkins T. W., Miller E. E. and Chance B., "Correlation between the light scattering and the mitochondrial content of normal tissues and transplantable rodent tumor," Analytical Biochemistry 226, 167-174 (1995).
[13] Arismendi-Morillo G., "Electron microscopy morphology of the mitochondrial network in gliomas and their vascular microenvironment," Biochimica et Biophysica Acta (BBA) - Bioenergetics 1807(6), 602-608 (2011).
[14] Oudard S, Boitier E, Miccoli L, Rousset S, Dutrillaux B, Poupon MF., "Gliomas are driven by glycolysis: putative roles of hexokinase, oxidative phosphorylation and mitochondrial ultrastructure," Anticancer Res. 17(3C), 1903-1911 (1997).
[15] Huang Z., Jiang J., Belikova N. A., Stoyanovsky D. A., Kagan V. E. and Mintz A. H., "Protection of normal brain cells from γ-irradiation-induced apoptosis by a mitochondria-targeted triphenyl-phosphonium-nitroxide: a possible utility in glioblastoma therapy," Journal of Neuro-Oncology 100 (1), 1-8 (2010).
[16] Valdes P. A., Leblond F., Kim A., Harris B. T., Wilson B. C., Fan X., Tosteson D., Hartov A., Ji S., Erkmen K., Simmons N. E, Paulsen K. D. and Robert D. W., "Quantitative fluorescence in intracranial tumor: implications for ALA-induced PpIX as an intraoperative biomarker," J Neurosurg 115, 11-17 (2011).
[17] Schmitt J.M. and Kumar G., "Turbulent nature of refractive-index variations in biological tissue," Opt. Lett., 21(16), 1310-1312 (1996).
[18] Schmitt J.M. and Kumar G., "Optical scattering properties of soft tissue: a discrete particle model," Appl. Opt. 37(13), 2788-2797 (1998).
[19] Wilson J. D., Foster T.H., "Mie theory interpretations of light scattering from intact cells," Optics Letters 30(18), 2442-2444 (2005).
[20] Beauvoit B., Kitai T. and Chance B., "Contribution of the mitochondrial compartment to the optical propertires of the rat liver: a theoretical and practical approach," Biophys. J. 67, 2501-2510 (1994).
[21] Beauvoit B. and Chance B., "Time-resolved spectroscopy of mitochondira, cells and tissues under normal and pathological conditions", Mol. Cell. Biochem., 184(1-2), 445-455 (1998).
[22] Barer R. and Joseph S., ''Refractometry of living cells,'' Quart. J. Microscop.Sci. 95, 399-423 (1954).
[23] Dunn A., Smithpeter C., Welch A J, Richards-Kortum R, "Finite-difference time-domain simulation of light scattering from single cells," Journal of Biomedical Optics, 2(3), 262-266 (1997).
[24] Backman V., Gurjar R., Badizadegan K., Itzkan I., Dasari R. R., Perelman L. T. and Feld M. S "Polarized light scattering spectroscopy for quantitative measurement of epithelial structures in situ," IEEE J. Sel. Topics Quant. Elec. 5(4), 1019-1026 (1999).
[25] Beuthan J., Minet O., Helfmann J., Herrig M., Muller G., "The spatial variation of the refractive index in biological cells," Phys Med Biol 41(3), 369-382 (1996).
[26] Backman V., Wallace M. B., Perelman L. T., Arendt J. T., Gurjar R., G.Muller M., Zhang Q., Zonios G., Kline E., McGilligan J. A., Shapshay S., Valdez T., Badizadegan K., Crawford J. M., Fitzmaurice M., Kabani S., Levin H. S., Seiler M., Dasari R. R., Itzkan I., van Dam J. and Feld M. S., "Detection of preinvasive cancer cells," Nature 406, 35-6 (2000).
[27] Johansen-Berg H. and Behrens T. E.-G., [Diffusion MRI: from quantitative measurement to in vivo neuroanatomy], Ac. Press. Elsevier, China, 75-126, (2009).
[28] Brady S. T., Siegel G. J., Alberts R. W. and Price D. L., [Basic Neurochemistry: Principles of Molecular, Cellular and Medical Neurobiolog, 8th ed.], Ac. Press. Elsevier, China, 185 (2011).
[29] Mourant J.R., Boyer J., Hielscher A.H., and Bigio I.J., "Influence of the scattering phase function on light transport measurements in turbid media performed with small source-detector separations," Opt. Lett., 21(7), (1996).
[30] Canpolat M., Mourant J.R., "High-angle scattering events strongly affect light collection in clinically relevant measurement geometries for light transport through tissue," Phys. Med. Biol. 45, 1127-1140, (2000).
[31] LeBihan D., Mangin J.-F., Poupon C., Clark C. A., Pappata S., Molko N. and Chabriat H., "Diffusion tensor imaging: concepts and applications," J Magn Reson Imaging; 13, 534-546 (2001).
[32] Mie G., "Beiträge zur Optik trüber Medien, speziell kolloidaler Metallösungen," Ann. Phys. 330(3), 377-445 (1908).
[33] Antonov I. P., Goroshkov A. V., Kalyunov V. N., Markhvida I. V., Rubanov A. S., and Tanin L.V., "Measurement of the radial distribution of the refractive index of the Schwann's sheath and the axon of a myelinated nerve fiber *in vivo*," J. Appl. Spectrosc., 39(1), 822-824 (1983).

[34] Hilderband C., Remahl S., Persson H., Bjartmar C., "Myelinated nerve fibers in the CNS," Prog. Neurobiol 40, 421-434 (1993).
[35] Brusting A. and Mullaney P., "Differential light scattering from spherical mammalian cells," Biophysical Journal, 14, 439-453 (1974).
[36] Cataldo A. M., McPhie D. L., Lange N.T., Punzell S., Elmiligy S., Ye N. Z., Froimowitz M. P., Hassinger L. C., Menesale E. B., Sargent L. W., Logan D. J., Carpenter A.E. and Cohen B. M., "Abnormalities in Mitochondrial Structure in Cells from Patients with Bipolar Disorder," The American Journal of Pathology 177 (2), 575-585 (2010).
[37] von Keyserlingk G., Schramm U., "Diameter of axons and thickness of myelin sheaths of the pyramidal tract fibres in the adult human medullary pyramid," Anat Anz.,157(2), 97-111 (1984).
[38] Evangelou N., Konz D., Esiri M. M., Smith M., Palace J., Matthews P. M., "Size-selective neuronal changes in the anterior optic pathways suggest a differential susceptibility to injury in multiple sclerosis," Brain 124, 1813-1820 (2001).
[39] Biedenbach M. A., De Vito J. L, Brown A. C., "Pyramidal tract of the cat: axon size and morphology," Exp Brain Res. 61, 303-310 (1986).
[40] Rushton W. A., "A theory of the effects of fibre size in modulated nerve," J. Physiol 115(1), 101-122 (1951).
[41] Rappaz B., Marquet P., Cuche E., Emery Y., Depeursinge C. and Magistretti P. J., "Measurement of the integral refractive index and dynamic cell morphometry of living cells with digital holographic microscopy," Optics Express 13(23), 9361-9373. (2005).
[42] Tuchin V. V., [Tissue optics:light scattering methods and instruments for medical diagnosis, 2nd ed.], SPIE Press, USA, 148-157 (2007).